

Published Approaches to InSAR Time Series

David Sandwell, *Scripps Institute of Oceanography*

28 January 2016

Schmidt and Burgman, JGR 2003

Time-dependent land uplift and subsidence in the Santa Clara valley, California, from a large interferometric synthetic aperture radar data set

Lanari, Lungren, Manzo, & Casu, GRL 2004

Satellite radar interferometry time series analysis of surface deformation for Los Angeles, California

Ozawa and Ueda, JGR, 2011

Advanced interferometric synthetic aperture radar (InSAR) time series analysis using interferograms of multiple-orbit tracks: A case study on Miyake-jima

Schmidt and Burgman, JGR 2003

Time-dependent land uplift and subsidence in the Santa Clara valley, California, from a large interferometric synthetic aperture radar data set

InSAR Processing

- 115 interferograms from ERS-1/2, 1992 – 2000
- descending only because only 9 ascending available – assume vertical
- baselines < 200 m
- boxcar filtering to 150 m pixels + Goldstein & Werner adaptive filter
- removed a regional gradient from dislocation model based on GPS
- unwrapped phase with “bridges” to connect islands
- flattened residual with plane
- referenced zero to Oak Hill Outcrop

Notes: “The ERS spacecraft repeat their orbits every 35 days; however, longer gaps occur when acquisitions were not scheduled, orbit baselines were un-suitable, or the spacecraft orbital configuration was altered.”

Time Series Approach – also called SBAS (Berardino et al., 2002)

d_i – InSAR displacement between two times

m_i – displacement increment

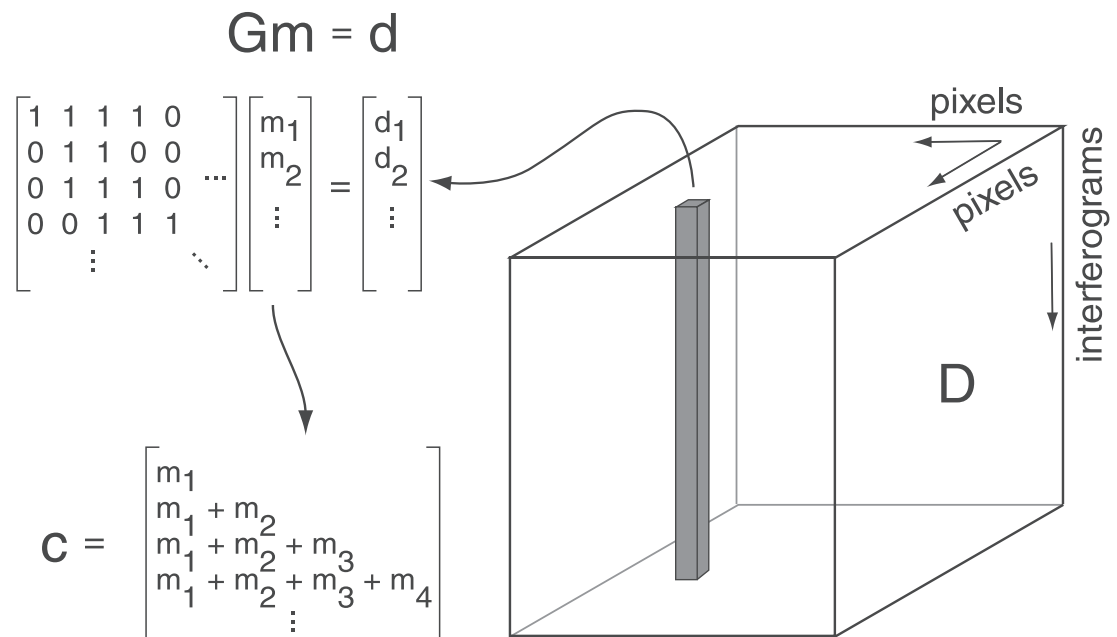
G – matrix maps m onto d

temporal smoothing by minimizing first difference of m_i

time series constructed by summing m_i

solved by SVD

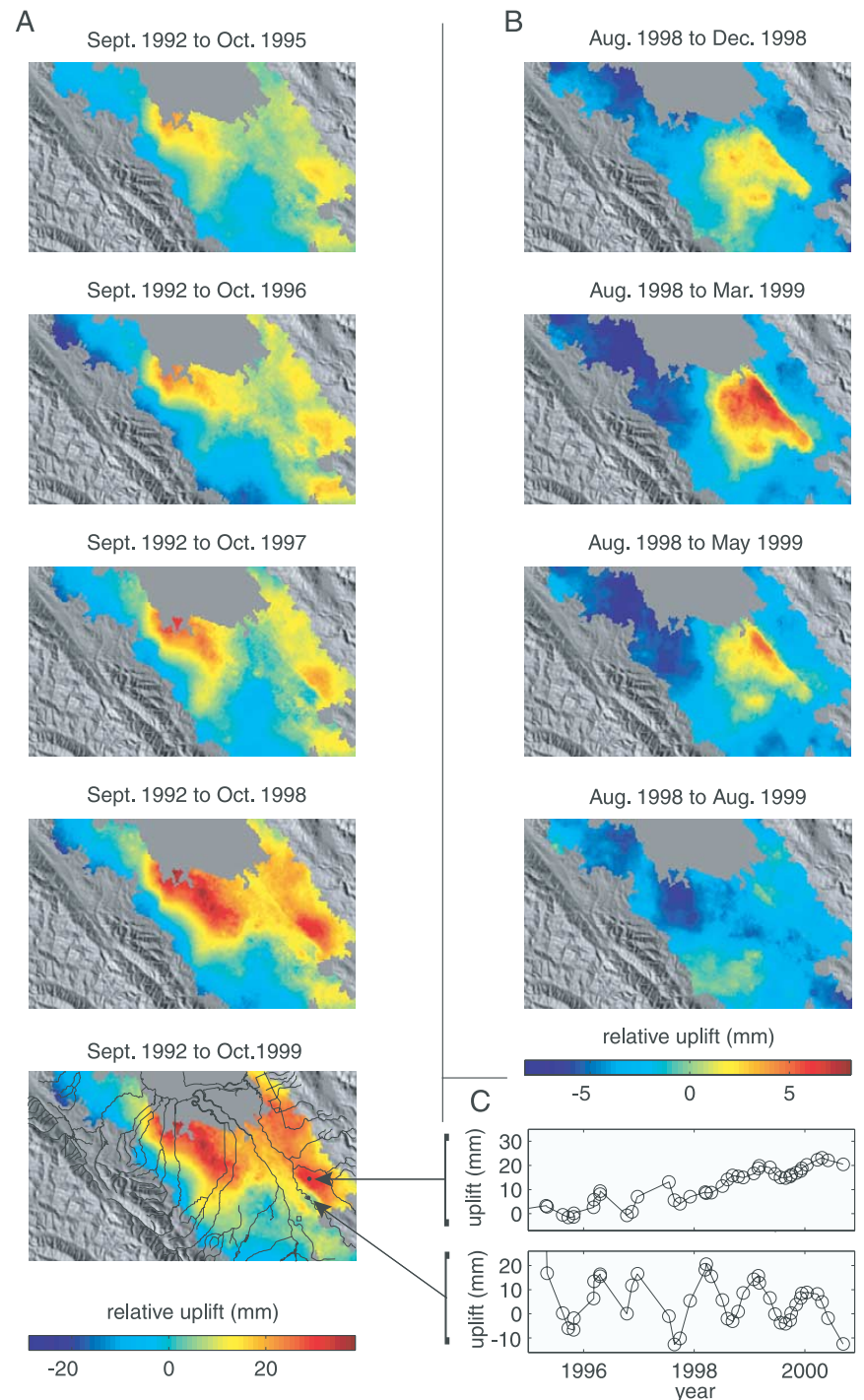
Note that InSAR subsets, in baseline-time space, may be disconnected so temporal smoothing/SVD provides the time connection.



Time Series Results

[Schmidt and Burgmann, 2003]

(a) Five frames from the InSAR time series show the pattern of cumulative uplift since September 1992 centered north of Sunnyvale and east of the Silver Creek fault near San Jose. Uplift is relative to Oak Hill (open square in final frame). The drainage network for the Santa Clara valley is also shown in the final frame. (b) Seasonal uplift pattern during a period from August 1998 to August 1999. (c) Comparison of time series at two points (dots in final frame of Figure 5a) illustrating the seasonal versus long-term deformation pattern partitioned by the Silver Creek.



Time Series Results

[Schmidt and Burgmann, 2003]

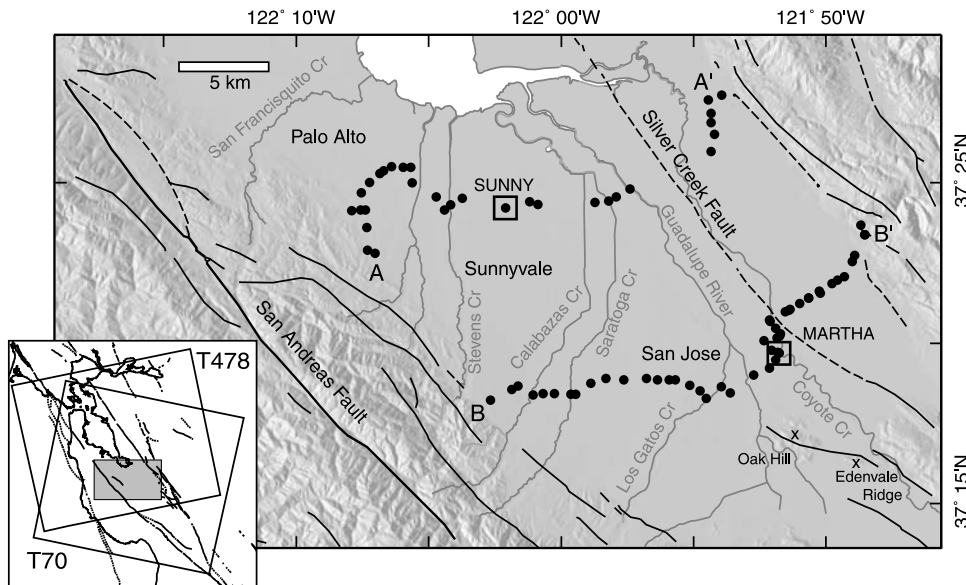


Figure 1. Shaded relief map of the Santa Clara valley. Bench mark locations are shown for two leveling lines (dots) and extensometer sites (open squares). All InSAR observations are referenced to Oak Hill. Faults appear as bold lines, dashed where inferred [Jennings, 1994]. Major drainage channels appear as gray lines. The inset shows the location of the Santa Clara valley (gray box) within the San Francisco Bay Area. The tilted rectangles identify the SAR frames along tracks 70 and 478.

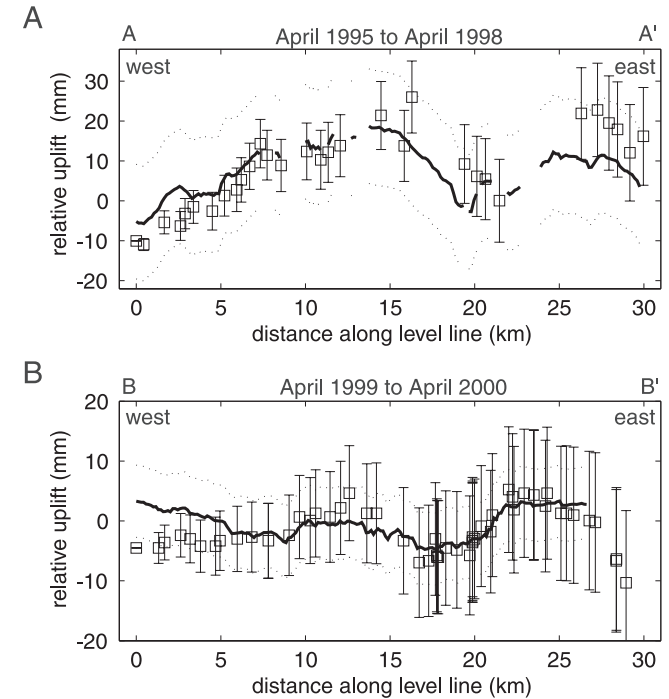


Figure 6. Comparison of leveling data (open squares with error bars) and the InSAR time series (solid line with dotted

Time Series Results

[Schmidt and Burgmann, 2003]

Conclusions:

“We demonstrate how a complex, time-dependent signal can be extracted from a large InSAR data set. Our time series methodology does not parameterize the mode of deformation, whether it be linear, nonlinear, or sinusoidal. The inversion also acts to reduce atmospheric and orbital artifacts inherent in each individual interferogram.”

“The temporal and spatial pattern of uplift and subsidence afforded by InSAR provides important constraints on the lateral distribution of water-bearing units and the time scales over which the groundwater is exchanged. A higher transmissivity allows for the rapid redistribution of groundwater beneath San Jose resulting in a large, seasonal deformation signal.”

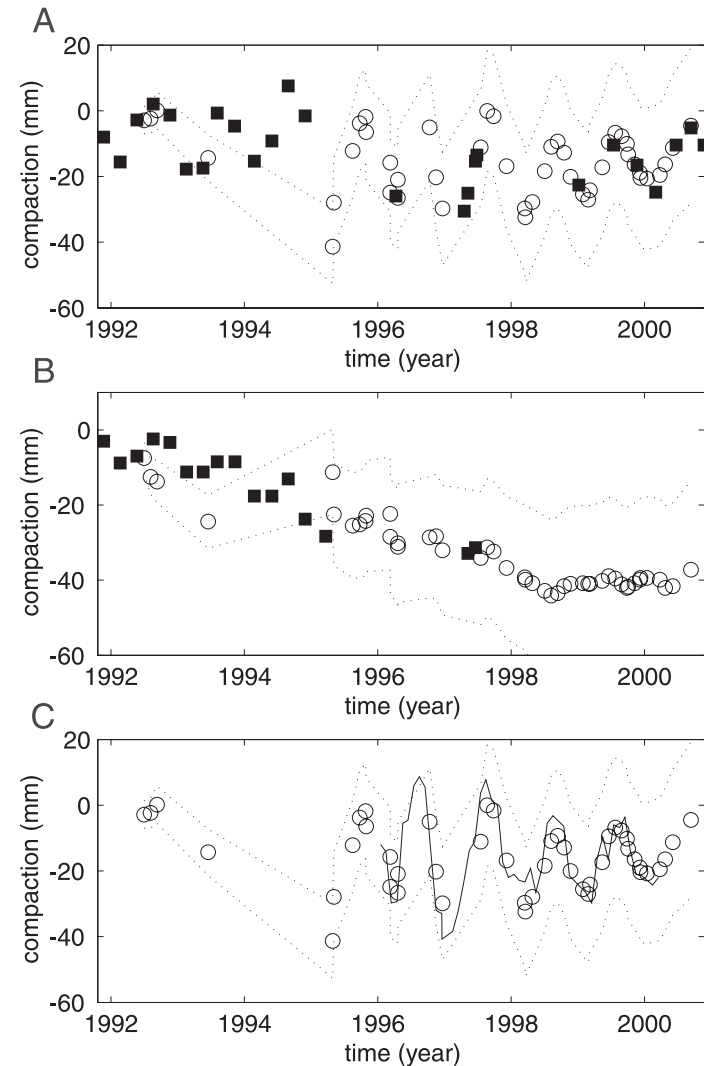


Figure 7. Comparison of extensometer observations (solid squares) and the InSAR time series (circles with dotted error envelope) for instruments (a) MARTHA and (b) SUNNY. (c) Comparison of the InSAR time series to well level depths that have been converted to compaction using the

Lanari, Lungren, Manzo, & Casu, GRL 2004

Satellite radar interferometry time series analysis of surface deformation for Los Angeles, California

InSAR and Time Series Processing

- 102 interferograms from ERS-1/2, 1995 – 2002
- descending only assume vertical
- baselines < 300 m
- unwrapped phase
- flattened residual with plane
- SBAS time series analysis
- No explicit connection to GPS

Time Series Results

[Lanari et al., 2004]

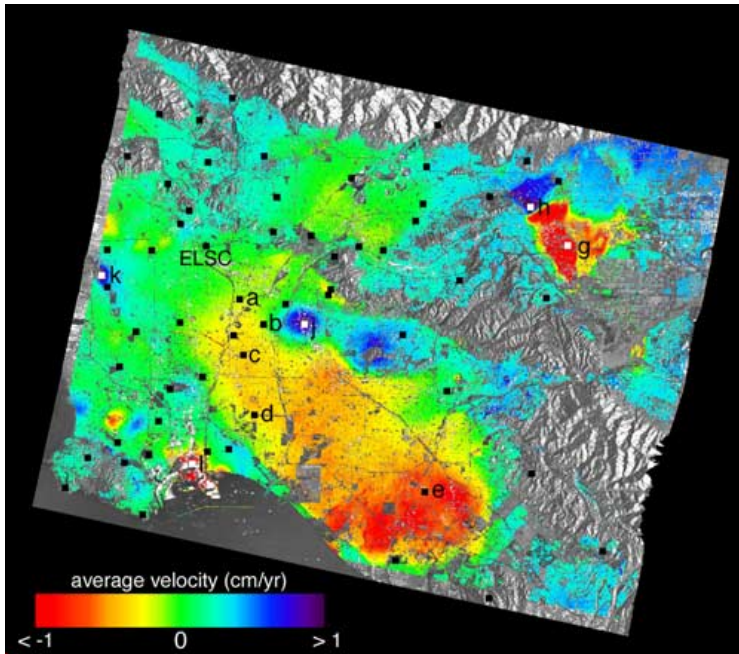
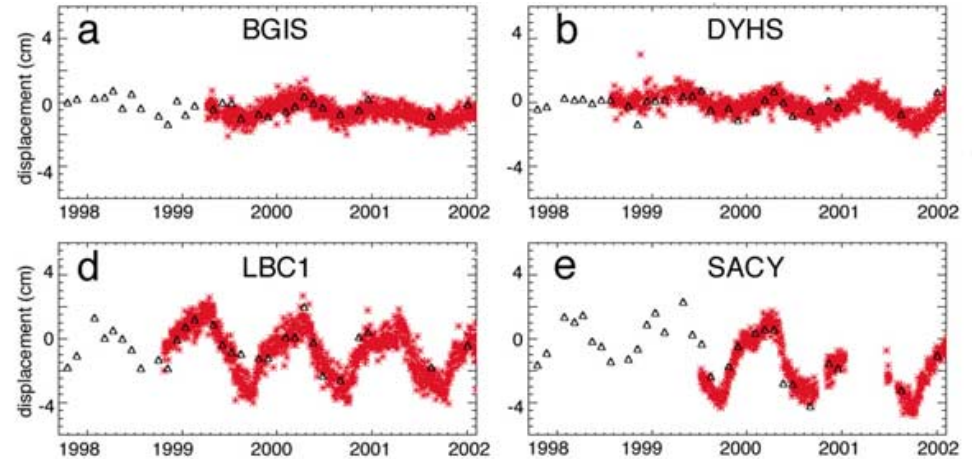


Figure 2. InSAR mean LOS deformation velocity map, overlying the SAR amplitude image. Small black squares mark SCIGN GPS site locations. Those marked *a* through *e* correspond to their respective time series plots in Figure 3. ELSC marks the time series reference point. White squares mark the locations of plots *g*, *h*, *j*, *k*, *l* in Figures 3.



“The InSAR time series reveals ground water related surface deformation that occurs on two different time scales reflecting different processes in the Santa Ana basin.

The longer timescale subsidence (Figure 2) is consistent with aquitard drainage models in which inelastic compaction occurs that is incompletely compensated by elastic expansion during winter recharge .

The second time scale relates to the annual recharge of the basin (Figures 3 and 4) and the fluid dynamics of flow, as reflected in the spatial distribution of the phase delay of maximum uplift.”

Ozawa and Ueda, JGR, 2011

Advanced interferometric synthetic aperture radar (InSAR) time series analysis using interferograms of multiple-orbit tracks: A case study on Miyake-jima

InSAR and Time Series Processing

- ascending **and** descending look directions constrain E-W and U-D deformation but NOT N-S.
- 232 interferograms from ALOS-1, 2006 – 2011
- baselines < 2000 m
- filtered with adaptive Goldstein & Werner – 64 X 64
- unwrapped phase
- atmospheric delay corrected with 10 km weather model
- flattened residual with plane and fit to 11-day averages of GPS
- SBAS-like time series analysis but accommodates multiple LOS directions to solve for EW and UD

Time Series Results

[Ozawa and Ueda 2011]

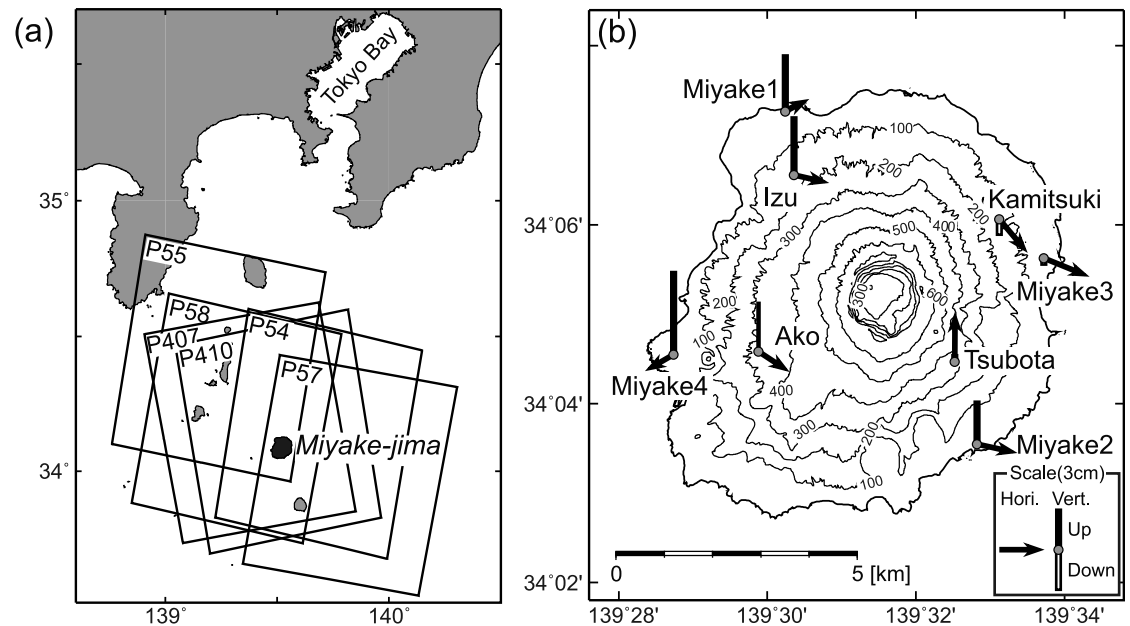


Figure 3. (a) Map of the area around Miyake-jima, the target of the case study. Rectangles denote PALSAR frames used in this study. (b) Topographic map of Miyake-jima and GPS displacements for 12 June 2006 and 8 August 2010.

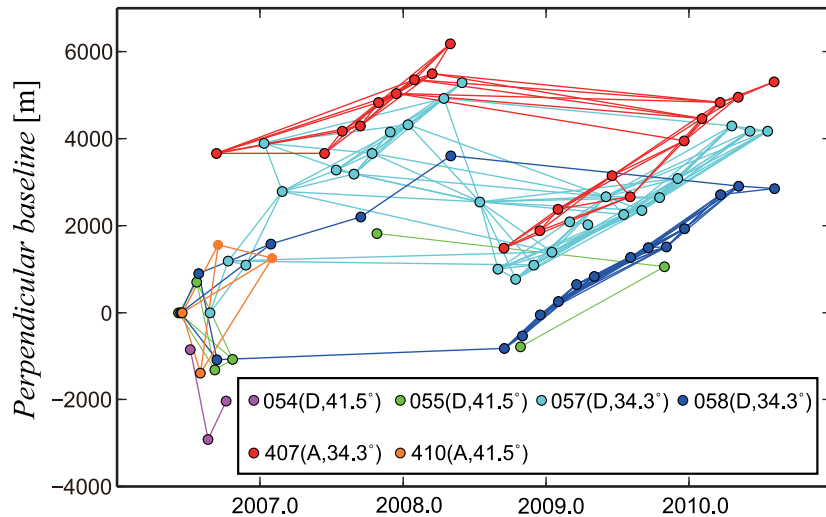


Figure 4. Diagram of perpendicular baselines and interferometric pairs.

Time Series Results

[Ozawa and Ueda 2011]

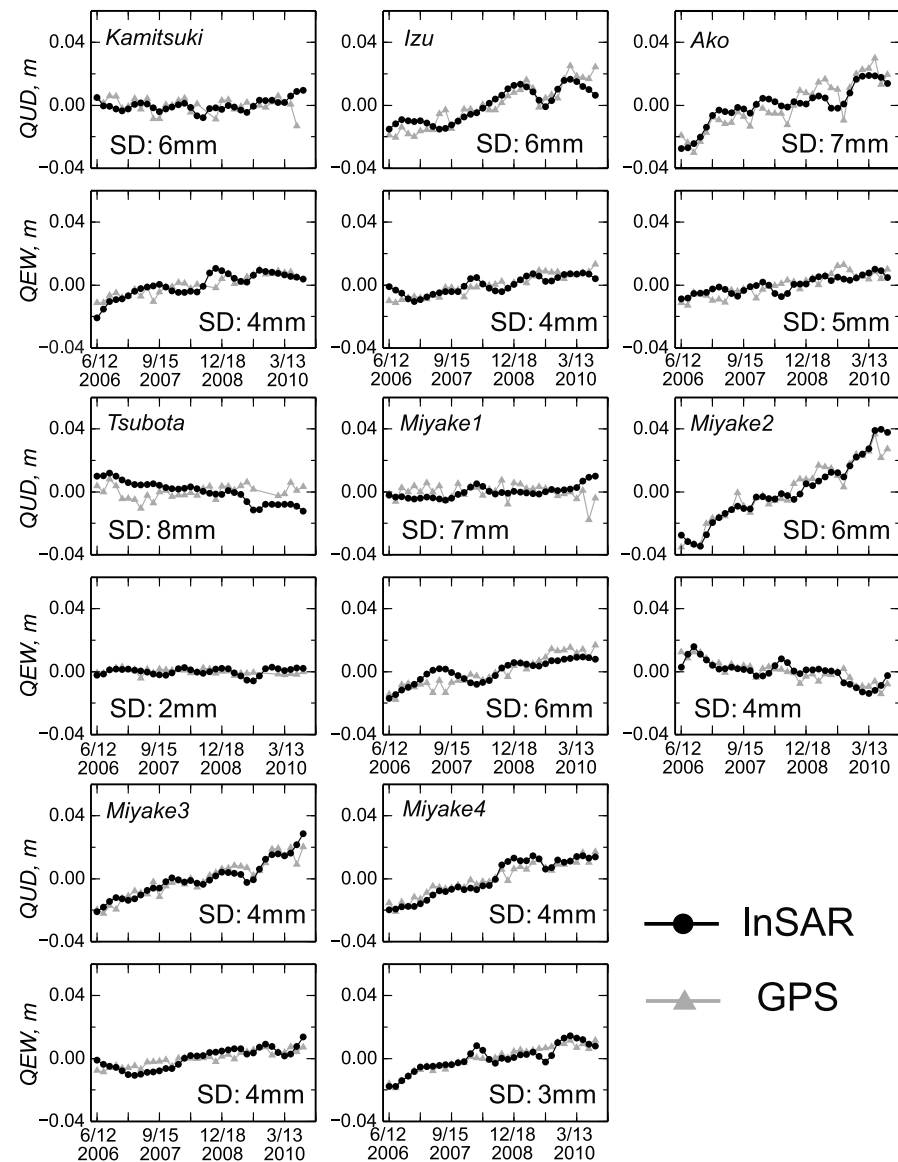
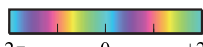
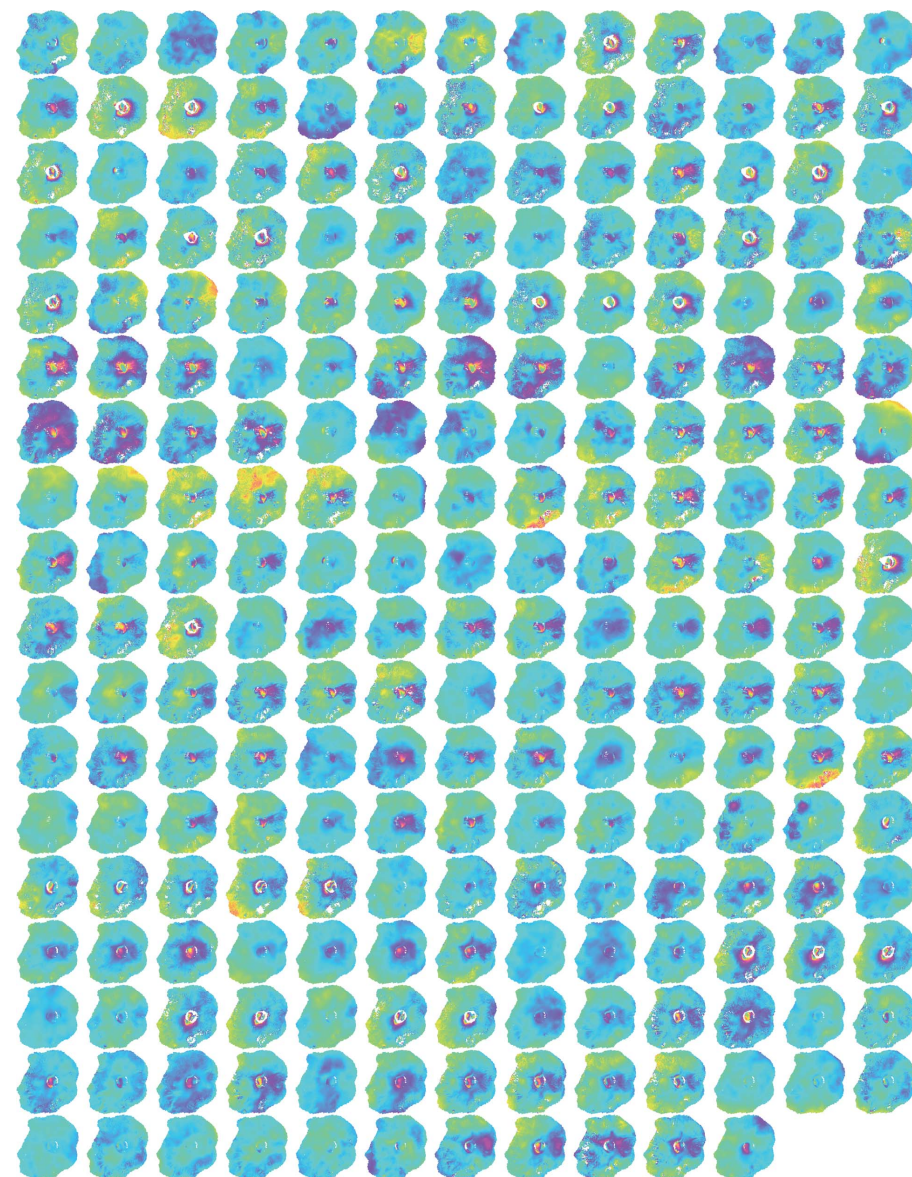


Figure 8. Comparison of time series by the advanced InSAR time series analysis (solid circles) and GPS (gray triangles).

Conclusions

[Ozawa and Ueda 2011]

“In this paper, we propose an advanced InSAR time series analysis that estimates two components of a deformation time series in the best-fit plane of all incidence angles from interferograms of multiple-orbit tracks. One advantage of this analysis is improvement of accuracy using SAR data of multiple-orbit tracks. Another advantage is that interferograms for different incidence directions can be integrated. “

Overall Conclusions and Questions

- Most studies of natural targets use standard InSAR processing, filtering, unwrapping, and SBAS.
- Spatial and temporal filtering (e.g., wavelets, MINTS, etc.) are needed to reduce atmosphere/ionosphere and orbital effects.
- The older data sets do not usually have the baseline control or cadence to resolve the annual signal.
- How should we filter the dense GPS time series to connect with sparse InSAR time series? What about events?
- Should we project vector GPS into the LOS or the E-W, U-D coordinates?
- Should we use a block model to connect GPS and InSAR at the large scale or in areas of high strain rate?